GEOPHYSICAL RESEARCH LETTERS, VOL. 40, 167–172, doi:10.1029/2012GL054457, 2013

A unique seasonal pattern in dissolved elemental mercury in the South China Sea, a tropical and monsoon-dominated marginal sea

C. M. Tseng,[1] C. H. Lamborg,[2] and S. C. Hsu[3]

Received 1 November 2012; revised 29 November 2012; accepted 3 December 2012; published 16 January 2013.

[1] A unique seasonal pattern in dissolved elemental mercury (DEM) was observed in the tropical monsoon-dominated South China Sea (SCS). The DEM concentration varied seasonally, with a high in summer of 160 ± 40 fM (net evasion 580 ± 120 pmol m^{-2} d^{-1}, $n = 4$) and a low in winter of 60 ± 30 fM (net invasion −180 ± 110, $n = 4$) and showed a positive correlation with sea surface temperature (SST). The elevated DEM concentration in summer appears mainly abiologically driven. In winter, the SCS acts as a sink of atmosphere Hg^0 as a result of low SST and high wind of the year, enhanced vertical mixing, and elevated atmospheric gaseous elemental mercury. Annually, the SCS serves as a source of Hg^0 to the atmosphere of 300 ± 50 pmol m^{-2} d^{-1} (385 ± 64 kmol Hg yr^{-1}, ~2.6% of global emission in ~1% of global ocean area), suggesting high regional Hg pollution impacts from the surrounding Mainland (mostly China). **Citation:** Tseng, C. M., C. H. Lamborg, and S. C. Hsu (2013), A unique seasonal pattern in dissolved elemental mercury in the South China Sea, a tropical and monsoon-dominated marginal sea, *Geophys. Res. Lett.*, *40*, 167–172, doi:10.1029/2012GL054457.

1. Introduction

[2] Mercury (Hg) is a neurotoxic element present in nature with a fascinating biogeochemical cycle. During the past decades, we have learned much about the global cycling of Hg and interactions affecting its exchange at surface interfaces, e.g., air-water [*Mason et al.*, 1994; *Lamborg et al.*, 2002; *Selin et al.*, 2008; *Soerensen et al.*, 2010]. The results demonstrate the ocean plays a crucial role in the global cycle of Hg, representing about 30% of the total emissions of Hg to the atmosphere. However, the role of marginal seas in Hg emissions on a global scale has not yet been widely recognized. The evasion of Hg in some marginal seas have been summarized [*Coquery and Cossa*, 1995; *Wangberg et al.*, 2001; *Gårdfeldt et al.*, 2003; *Balcom et al.*, 2004; *Fu et al.*, 2010; *Ci et al.*, 2011], mostly from European (e.g., Mediterranean Sea, North Sea, Baltic Sea), and U.S. waters (e.g., the mid-Atlantic Bight, Long Island Sound) and a few from East Asian waters (e.g., South China Sea, Yellow Sea, Tokyo Bay). These studies indicate that overall, marginal seas are a source of Hg^0 to the atmosphere (are supersaturated). The evasion rate in these studies ranged from 20 to 1000 pmol m^{-2} d^{-1} and depended on the differences of latitude and locality related to human activities. Generally, marginal seas in the Northern Hemisphere (e.g., Baltic Sea, Mediterranean Sea) exhibit higher fluxes of Hg^0 than the open ocean at the same latitude (averaged ~130 pmol m^{-2} d^{-1}; between 10°N and 50°N). This trend suggests a disproportionate importance for marginal seas as a global source of atmospheric Hg, despite their relatively small total surface area (~8% of the whole ocean area). Further, limited knowledge exists concerning the role of the tropical-subtropical and monsoon-dominated marginal seas in East Asia in regulating the Hg air-sea flux such as South China Sea (SCS).

[3] The SCS is adjacent to the largest atmospheric Hg emission source region in the world (e.g., East Asian continent, particularly Mainland China, and Indochina peninsula) [*Pacyna et al.*, 2010]. Over the SCS, gaseous elemental Hg (GEM) concentrations are elevated 2–3 times above global background values, with higher enhancements in the winter when the northeast monsoon draws air from China [*Tseng et al.*, 2010; *Tseng et al.*, 2012]. The elevated atmospheric concentrations over this marginal sea give rise to higher deposition loadings and thereby enhance the opportunity for Hg transformation (e.g., methylation and reduction) in ecosystems. However, much of this elevated loading may be recycled through evasion, thereby spreading the potential reach of East Asian emissions to the regional and even global level.

[4] To assess this potential mobilization of Hg through air-sea gas exchange, we have determined the dissolved elemental Hg (DEM) and GEM concentrations in surface seawater and atmosphere, respectively, during seasonal oceanographic cruises to the Southeast Asian Time-series Study (SEATS) station (18°N, 116°E; Figure 1) from 2003 to 2007. We have combined these concentration data with meteorological and hydrographic variables as well as a simple box model to examine the time series variability in DEM with its air-sea exchange flux in the SCS. In this study, we present the first data set to show seasonal DEM variations in the SCS. This data set shows a unique seasonal cycle and flux of Hg^0, changing from a Hg sink in winter to a source in summer. The data set offers an opportunity to study the potential controlling mechanisms and sources of Hg associated with seasonal SST and monsoon cycle from East Asian Mainland in a low-latitude tropical marginal sea.

2. Materials and Methods

[5] The SCS (Figure 1) is the largest semi-enclosed marginal sea in the western North Pacific. It covers an area of

All Supporting Information may be found in the online version of this article.

[1]Institute of Oceanography, National Taiwan University, Taipei, Taiwan.
[2]Woods Hole Oceanographic Institution, Woods Hole, Massachusetts, USA.
[3]Research Center for Environmental Changes, Academia Sinica, Taipei, Taiwan.

Corresponding authors: C. M. Tseng, Institute of Oceanography, National Taiwan University, PO Box 23-13, Taipei 106, Taiwan. (cmtseng99@ntu.edu.tw)
C. H. Lamborg, Woods Hole Oceanographic Institution, MS 51, Woods Hole, MA 02543, USA. (clamborg@whoi.edu)

0094-8276/13/2012GL054457

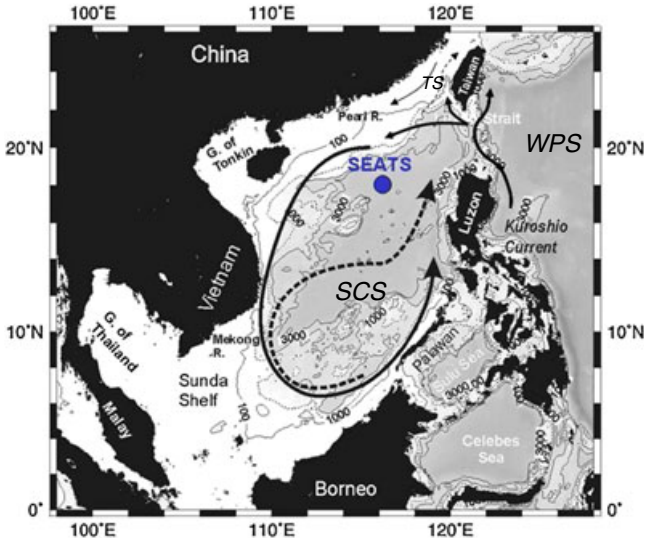

Figure 1. The location of the SEATS station in the SCS. Solid line is the cyclonic gyre in the winter whereas dashed line is the anti-cyclonic gyre. The flow path of the Kuroshio and its intrusion into the South China Sea are also shown. TS, Taiwan Strait; WPS, West Philippine Sea; SCS, South China Sea.

3.5×10^6 km^2 with an average depth of 1200 m and lies entirely within the tropical zone. The SEATS station was occupied with on-board atmospheric and water Hg sampling 16 times between May 2003 and January, 2007 in approximately seasonal intervals aboard R/V *Ocean Researcher-I* and *Fishery Researcher-1*. Methods used in this study for data sampling, analyses, and assurances regarding Hg [*Tseng et al.*, 2003, 2010] and hydrographic variables [*Tseng et al.*, 2005, 2007] are described in detail in the Supporting Information.

[6] Percent saturation (%S) of DEM (i.e., DEM in the SCS seawater relative to that calculated to be in equilibrium with the atmospheric GEM) is determined with the following equation: $\%S = [(DEM \times H)/GEM] \times 100$, where DEM and GEM are the concentrations measured in surface seawater and in the overlying air, respectively. H represents the dimensionless Henry's law constant of Hg^0, adjusted for sample temperature and salinity [*Andersson et al.*, 2008]. Values of $\%S > 100$ are commonly observed and indicate supersaturation and the potential for transfer of Hg^0 from surface water to air.

[7] The exchange flux, F, of Hg^0 at the air-seawater interface is given by $F = K \times (DEM - GEM/H)$, where F (pmol m^{-2} d^{-1}) is the volatile Hg^0 flux into (−) or out (+) of the SCS. The formulation we used for the transfer velocity was K (m d^{-1}) = $0.39\,u^2(Sc^T_{Hg}/600)^{-1/2}$, developed by *Wanninkhof* [1992] for use with average winds. The u^2 term is the squared mean wind velocity at 10 m height (m^2 s^{-2}), and Sc is the temperature- and salinity-dependant dimensionless Schmidt number for Hg^0 at a given temperature T, estimated from the variation of Sc values of other gases as a function of molecular weight [*Wanninkhof*, 1992]. The constant value of 0.39 is empirically derived. Numerous other parameterizations for the K value exist, a popular one of which is that of *Nightingale et al.* [2000]. This formulation also makes use of wind speed ($K = (0.222u^2 + 0.333u)(Sc^T_{Hg}/660)^{-1/2}$) and would result in about 65% lower fluxes at the wind speeds we report here. This would not affect the seasonality we describe and is likely within the uncertainty of gas exchange models in general, thus we report results based on the Wanninkhof model.

3. Seasonal Patterns in DEM and Related Environmental Conditions

[8] Temporal variations in DEM and GEM and environmental variables in the SCS surface from May 2003 to January 2007 are presented in Figure 2, and all data show distinctive seasonal patterns. Detailed descriptions in surface dynamics of seasonal variability were mentioned by *Tseng et al.* [2005; 2007]. Briefly, the SCS surface water is warm year-round with a summer maximum of 28–31°C and winter minimum of 23–26°C (Figure 2a). The wind pattern was governed by the monsoons: winter northeast monsoon with higher wind speed (WS; averaged ~10 m s^{-1}), summer southwest monsoon with weaker WS (averaged ~6 m s^{-1}) and lower WS (<5 m s^{-1}) in the inter-monsoonal periods in April–May and September–October (Figure 2b). The upper water column is well stratified at all times, but vertical mixing is promoted in winter due to surface cooling and strong northeast monsoon winds. As a result, the mixed layer depth (MLD) increased from 20 m in the summer to 60–100 m in the winter. Also, high

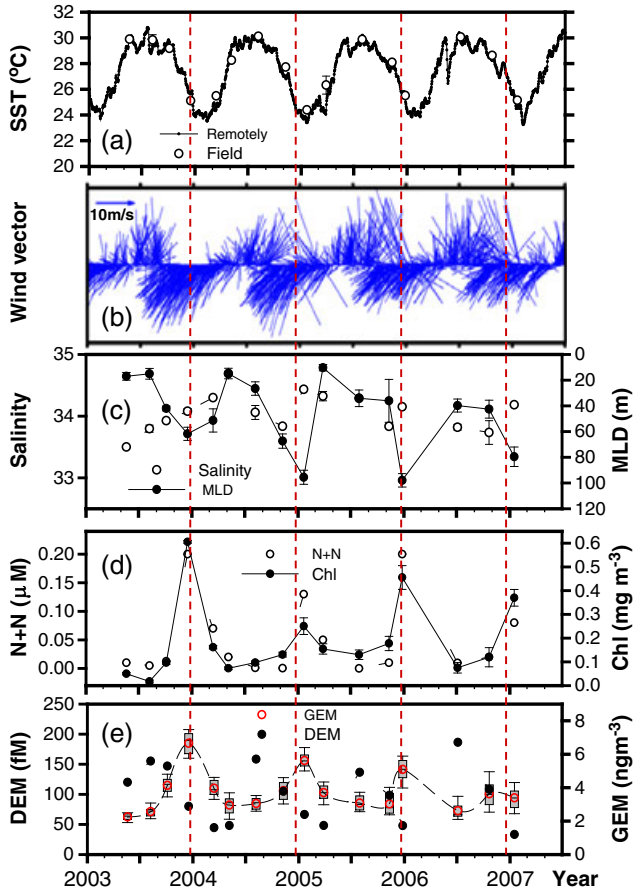

Figure 2. Time series of records obtained for the SEATS station in the SCS between 2003 and 2007. (a) Remotely sensed sea surface temperature (SST, solid circle) and field observed SST (field, open circle); (b) remotely sensed wind vector; (c) mixed layer depth (MLD, solid circle) and salinity (S, open circle); (d) averaged mixed-layer Chl-*a* (solid circle) and (N + N) (open circle); and (e) averaged DEM (solid circle) and GEM (open circle).

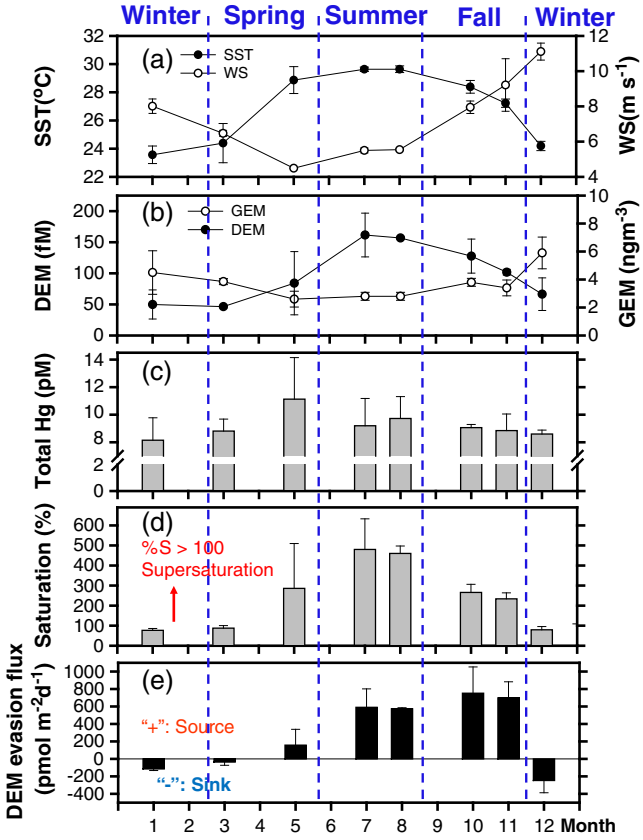

Figure 3. Monthly average data (with ±1 SD) for (a) SST and WS; (b) DEM and GEM; (c) total Hg; (d) saturation (%); and (e) air-sea Hg^0 exchange flux between 2003 and 2007 at the SEATS station in the SCS.

salinity (34.2) and maximum concentrations in nitrate + nitrite (N + N; 0.2 μM) and Chl-*a* (0.4 mg m^{-3}) in the mixed layer were found in winter (Figures 2c and 2d). The wind-reinforced convective overturn enhanced vertical mixing between the fresher surface water and the more saline subsurface Tropical Water, which appeared as the salinity maximum (34.6‰) centered around 150 m and also brought nutrients to the mixed layer, stimulated primary production [*Tseng et al.*, 2005] and led to the distinct seasonal maximum in Chl-*a* in winter.

[9] Seasonal DEM pattern in the surface seawater was slightly out of phase relative to that of GEM (Figure 2e). There was a winter maximum of the GEM (3.4–5.9 ng m^{-3}) associated with northeast wind and a minimum (2.2–3.0 ng m^{-3}) in late spring and summer with southward wind (Figure 2e) with an annual mean of 3.5 ± 0.2 ng m^{-3}. We previously asserted that seasonal variation of GEM is influenced by the sources of GEM, i.e., the sources of air masses governed by the monsoon cycling and the observation that air masses from Mainland China contain high Hg [*Tseng et al.*, 2012].

[10] The opposing seasonal trends in DEM and GEM indicate that DEM seasonality is not determined by the seasonal GEM changes or mechanisms controlling the GEM variations. Instead, the variations in DEM stayed closely in phase with those in SST (Figures 2a, 2e, 3a, and 3b), which may modulate the formation of DEM. Thus, DEM was at a minimum in winter (~30 fM) and increased progressively through the spring and reached a maximum of ~200 fM in summer before it retreated steadily through the fall back to a minimum value in winter. A linear relationship between DEM and SST in the mixed layer was observed during the study period such that $[DEM](\mathrm{fM}) = 16.7\ (\pm 2.2) \times [SST]\ (^\circ\mathrm{C}) - 346\ (\pm 60)$, $r^2 = 0.81$, $n = 16$. Although the maximum GEM and the minimum DEM were both found in the winter, they were slightly offset from each other with the former occurring slightly ahead of the latter. The range in DEM in summer is similar to one previously observed in the northern SCS (average 180 ± 70 fM) [*Fu et al.*, 2010] and those for temperate marginal seas such as the eastern Mediterranean Sea (110–270 fM) [*Gårdfeldt et al.*, 2003], and slightly higher than those observed in the Baltic Sea (70–110 fM) [*Wangberg et al.*, 2001], the Tyrrhenian Sea (85–130 fM) [*Gårdfeldt et al.*, 2003]), and the Irish west coast (65–195 fM) [*Gårdfeldt et al.*, 2003].

4. Hg^0 Formation Mechanisms and Processes Controlling Seasonal DEM Variability

[11] We observed that seasonal variability in DEM was well correlated with SST ($r^2 = 0.81$, $n = 16$) other than for Chl-*a* and WS (Table S1), and this relationship offers an opportunity to explore some of the mechanistic controls behind Hg^0 formation in the SCS. The apparent activation energy (E_a, kJ mol^{-1}) of DEM production was calculated at 140 ± 20 kJ mol^{-1} for SST between 23°C and 31°C. This value is obtained from the slope of the linear regression of the natural logarithm of DEM concentration versus $1/T$ by using the Arrhenius equation: $K = Ae^{-Ea/RT}$, where K is the formation rate of Hg^0 (i.e., $[Hg^0]_i/[Hg^0]_{23}$) and E_a is the activation energy. This approach assumes that DEM concentration is a good proxy for its net production rate. The activation energy calculated in this way is similar to that estimated for surface waters in Swedish temperate lakes (about 125 ± 5 kJ mol^{-1} at water temperatures of 0.5–23°C) [*Xiao et al.*, 1991] and in Arctic lakes (about 150 ± 40 kJ mol^{-1} between 11°C and 15°C) [*Tseng et al.*, 2004]. This is a surprising finding given that the data are collected from very different systems that span a wide range of temperatures. The similarity in E_a expresses a common response that all the systems had to changing temperature, but all the water bodies had roughly similar DEM although widely differing temperatures. Thus, this seemingly universal value for E_a suggests a common sensitivity to changing temperature, but that overall Hg^0 concentrations are set by factors other than temperature.

[12] In addition to the calculation of activation energy, the temperature dependence of DEM in the SCS can be used to explore the mechanism of DEM production through the calculation of a Q_{10} value. The Q_{10} temperature coefficient is a measure of the rate of change of a biological or chemical system as a consequence of increasing the temperature by 10°C.

[13] This parameter, calculated as

$$Q_{10} = \left(\frac{k_2}{k_1}\right)^{\frac{10}{T_2 - T_1}},$$

tends to have a value of around 2–3 for biological reactions [*Valiela*, 1995] where k_1 and k_2 are the reaction rates at temperature T_1 and T_2, respectively. The apparent Q_{10} for DEM formation in the SCS is around 7, suggesting that this reaction is not directly biologically mediated. Clearly, the temperature dependence of Hg^0 formation shall be significantly important in all surface water bodies but requires more examination.

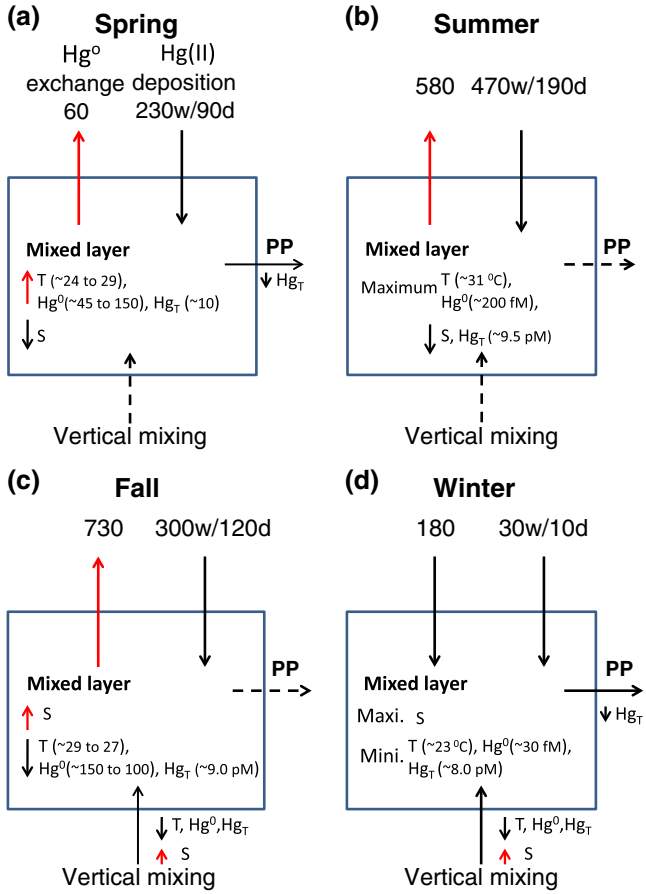

Figure 4. Conceptual diagram of the contributing processes to the changes in salinity, temperature and Hg in the mixed layer in (a) spring; (b) summer; (c) fall; and (d) winter. Observed changes in the mixed layer are shown in the box. Effects due to various processes are shown next to the arrows (flux unit: pmol m^{-2} d^{-1}). Thick solid line denotes major contributing process. Dashed line denotes minor process. w/d, atmospheric wet/dry deposition; up arrow, increase; down arrow, decrease.

[14] Further, the observed changes in DEM are related with seasonal SST changes in the mixed layer and major contributing processes together with their effects as shown in Figure 4 and Table S2. First, from spring (from March to May) to summer (June to August), the progressive surface heat gain accounted for the increase in SST (24°C to 29°C in spring; reaching maximum ~31°C in summer) and concomitant increase in DEM (~40 spring to ~200 fM summer) which led to supersaturation and favored the evasion of DEM to the atmosphere, thus switching the SCS from a sink to a source of Hg^0. This also coincided with a decrease in total Hg (Hg_T). Additionally, the Hg_T amount increased and reached maximum in spring (approximately 10 and 9.5 pM in summer; Figure 3c and Table S2) because a significant net input between evasion and atmospheric deposition (wet + dry) occurred. The increase in Hg_T from late winter to summer could have resulted from the increased Hg loading from atmospheric Hg(II) deposition and from the water column becoming increasingly stratified during this period.

[15] During the cooling period from summer to late fall, the observed variation in DEM could be accounted for by a combination of a net source of atmospheric Hg, and the increase vertical mixing with the Tropical Water as vertical stratification was weakened. As a result, SST (29–27°C), DEM (150–100 fM) and Hg_T (9.5–9 pM) all decreased. In this period of lower primary production and more limited vertical mixing, DEM changes still followed the changes in SST in the mixed layer. In fall, atmospheric inputs of Hg were similar to those in spring inputs into the SCS. However, there is a net evasion flux of Hg from the SCS to the atmosphere since the evasional Hg fluxes are higher than those deposited into the SCS from atmosphere.

[16] During the winter (December to February), the effects of surface heat loss and atmospheric Hg invasion and vertical mixing reached a maximum. We found that SST (23°C), DEM (30 fM), and Hg_T (8.0 p*M*) reached their minimum values while N + N (0.4 μm), Chl-*a* (0.2 mg m^{-3}) and primary production (300 mg C m^{-2} d^{-1}) [*Tseng et al.*, 2005, 2007] were at a maximum. Additionally, less atmospheric Hg inputs are associated with wet and dry fluxes of Hg(II) into the SCS. This mostly represents rain fluxes being lower during winter, relative to the summer monsoon. Its effect of lowering DEM and Hg_T had apparently been obscured by the effects of atmospheric deposition and air-sea exchange. Eventually, there is a Hg_T export, corresponding to the amount of atmospheric input (~220 pmol m^{-2} d^{-1}), from the mixed layer. This suggests that biological removal could play a major control in Hg decrease in winter. The estimated value is quite similar to that calculated by differences between annual atmospheric deposition and air-sea exchange of Hg as an average net input approximately 250 pmol m^{-2} d^{-1} to the SCS.

5. Air-Sea Exchange of DEM at the SEATS Station

[17] In the northern SCS, seasonal surface DEM (and its percent saturation, %*S*) ranged from 30 (70%) to 200 fM (600%) with an annual mean of 100 ± 20 f*M* (Figures 2e and 3d). DEM concentrations were higher in summer and autumn (160 ± 40 fM, 470 ± 110% saturation, $n = 4$, and 120 ± 30 fM, 250 ± 50% saturation, $n = 4$, respectively), while lower in spring and winter (70 ± 40 fM, 190 ± 160%, $n = 4$, and 60 ± 30 fM, 80 ± 10%, $n = 4$). Samples in early spring and winter were undersaturated with DEM (approximately 70–98%) relative to atmospheric equilibrium. Consequently, DEM evasion occurred in spring (60 ± 160 pmol m^{-2} d^{-1}), summer (580 ± 120), and autumn (730 ± 210) but reversed direction in winter (−180 ± 110; Figure 2d). Such a seasonal flux pattern has not been documented elsewhere and may be unique to the SCS, or perhaps to other marginal seas adjacent to industrial sources of Hg. It is also distinctly different from previous thoughts that there was no seasonal variation in Hg evasion fluxes from low-latitude tropical oceans [*Strode et al.*, 2007; *Fu et al.*, 2010].

[18] To our knowledge, this is the first data set to show a complete seasonal DEM distribution and flux. This assessment of annual flux in terms of better temporal coverage in this study is more reliable and representative. We observed the highest DEM in summer, but this did not translate into the highest evasion rates. According to the air-sea exchange estimates, evasion is controlled not only by DEM concentration but also by wind speed. The highest Hg evasion was obtained in fall because of higher wind speeds and then deepening of

the mixed layer in fall than summer, i.e., the exchange coefficient was larger during the period of evasion as a result of the stronger northeast monsoon in fall. The seasonal pattern shows a transition from source to sink in early winter (December) during the period of high GEM, low SST, and strong wind speed associated with the northeast monsoon (Figures 2 and 3). The weak sink status during cold periods is fairly sensitive to environmental changes, for instance, related to changes of SST by global warming and to disruption through human perturbations, further increasing the Hg emission from the SCS.

[19] Overall, the SCS annually serves as a net source of atmospheric Hg^0 of 300 ± 50 pmol m^{-2} d^{-1} (i.e., 110 ± 20 nmol m^{-2} yr^{-1}). The annual evasion from the whole SCS to the atmosphere averaged 385 ± 64 kmol Hg yr^{-1}, based on the 3.5×10^6 km^2 area of the SCS. This flux represents ~2.6% of the global emission of 14.7 Mmol yr^{-1} [*Soerensen et al*., 2010] in ~1% of global ocean area. This suggests an exceptionally high Hg emission rate compared to open oceans (2–3 times higher). It is interesting to note that if the SCS were representative of all continental shelf regions (8% of global ocean), then ocean margins would contribute about 20% of global Hg^0 evasion. However, the SCS is likely a stronger source of Hg^0 to the atmosphere than most marginal seas. The range of annual fluxes for the SCS is difficult to make a comparison with those in other marginal seas. That is because there are no complete annual data available and the published values are mostly focused on the warm seasons. However, and as we noted above, if we only compare the summer data in the SCS with other marginal seas, we found the summer flux data at the SEATS station tend to be higher than in many other locations. Higher emission rate in the SCS compared to other seas may be caused by high regional Hg inputs from surrounding countries via atmosphere. Based on a preliminary first-order mass balance of total Hg for the SCS, the atmospheric inputs (wet and dry deposition) of Hg to the SCS are the dominant ones relative to other sources (e.g., rivers, submarine groundwater discharge, and direct anthropogenic inputs) for the basin as a whole. That is because of the high volume of precipitation into the SCS (i.e., rain ~10,000 km^3/yr, being one-order larger than that from the Asian rivers ~1000 km^3/yr) and the basin-wide surface circulation gyres which effectively isolates the interior of the SCS proper from the influence of the land runoff. However, the roles of other input sources will be certainly worth elucidating in the future study.

6. Conclusions

[20] Through this study, we report the first data set to show a complete seasonal distribution and flux of the DEM at the SEATS station in tropical monsoon-dominated SCS. The main feature of this time series was summer maximum and winter minimum occurring as a result of seasonal changes in SST, wind speed, and atmospheric inputs. Overall, the SCS serves annually as a net source of atmospheric Hg^0 of 300 ± 50 pmol m^{-2} d^{-1} (i.e., 385 ± 64 kmol Hg yr^{-1}) with a source in warm seasons (summer 580 ± 120 pmol m^{-2} d^{-1}; autumn 730 ± 210) and a sink in cold seasons (winter -180 ± 110). The high Hg emission rate data imply that the SCS receives environmental pollution from the surrounding Mainland mostly via atmosphere. Further increasing Hg emission from the SCS may be fairly altered by environmental changes, for instance, related to changes of SST by global warming and to disruption through human perturbations. Therefore, the shift in the winter weak sink status will not be immediately apparent, but will emerge as a long-term trend amongst the year-to-year fluctuation. Persistent observation of the SCS should be continually conducted to investigate atmospheric cycling and air-sea exchange of Hg, which will be crucial for the assessment of potential changes in the future. As these interesting trends were only discovered as a result of repeated observations at a single station, this study is further evidence of the importance of conducting time series observations of Hg in ocean environments, with only one other similar study published to our knowledge [*Heimburger et al*., 2010].

[21] **Acknowledgments.** We thank captains and crews of the R/V *OR-I*. P. W. Chiang, Y. J. Wang, and C. S. Liu assisted in lab work. Support was provided by the National Science Council through grants NSC 97-2745-M-002-001-;98(99,100)-2611-M-002-013(014,004) and from the College of Science, National Taiwan University under the "Drunken Moon Lake Scientific Integrated Scientific Research Platform" grant, NTU 101R3252, as well as through the U.S. National Science Foundation under grant OCE-1132515 and 0928191.

References

Andersson, M. E., K. Gardfeldt, I. Wangberg, and D. Stromberg (2008), Determination of Henry's law constant for elemental mercury, *Chemosphere*, *73*, 587–592.

Balcom, P. H., W. F. Fitzgerald, G. M. Vandal, C. H. Lamborg, K. R. Rolfhus, C. S. Langer, and C. R. Hammerschmidt (2004), Mercury sources and cycling in the Connecticut River and Long Island Sound, *Mar. Chem.*, *90*(1–4), 53–74.

Ci, Z. J. et al. (2011), Distribution and air-sea exchange of mercury (Hg) in the Yellow Sea, *Atmos. Chem. Phys.*, *11*, 2881–2892, doi:10.5194/acp-11-2881-2011.

Coquery, M., and D. Cossa (1995), Mercury speciation in surface waters of the North Sea, *Neth. J. Sea. Res.*, *34*(4), 245–257.

Fu, X. W., et al. (2010), Mercury in the marine boundary layer and seawater of the South China Sea: Concentrations, sea/air flux, and implication for land outflow, *J. Geophys. Res. Atm.*, *115*.

Gårdfeldt, K., et al. (2003), Evasion of mercury from coastal and open waters of the Atlantic Ocean and the Mediterranean Sea, *Atmos. Environ.*, *37*, S73–S84.

Heimburger, L. E., D. Cossa, J. C. Marty, C. Migon, B. Averty, A. Dufour, and J. Ras (2010), Methyl mercury distributions in relation to the presence of nano- and picophytoplankton in an oceanic water column (Ligurian Sea, North-western Mediterranean), *Geochim. Cosmochim. Acta*, *74*(19), 5549–5559.

Lamborg, C. H., W. F. Fitzgerald, J. O'Donnell, and T. Torgersen (2002), A non-steady-state compartmental model of global-scale mercury biogeochemistry with interhemispheric atmospheric gradients, *Geochim. Cosmochim. Acta*, *66*(7), 1105–1118.

Mason, R. P., W. F. Fitzgerald, and F. M. M. Morel (1994), The biogeochemical cycling of elemental mercury—Anthropogenic influences, *Geochim. Cosmochim. Acta*, *58*(15), 3191–3198.

Nightingale, P. D., G. Malin, C. S. Law, A. J. Watson, P. S. Liss, M. I. Liddicoat, J. Boutin, and R. C. Upstill-Goddard (2000), In situ evaluation of air-sea gas exchange parameterizations using novel conservative and volatile tracers, *Global Biogeochem. Cy.*, *14*(1), 373–387.

Pacyna, E. G., J. M. Pacyna, K. Sundseth, J. Munthe, K. Kindbom, S. Wilson, F. Steenhuisen, and P. Maxson (2010), Global emission of mercury to the atmosphere from anthropogenic sources in 2005 and projections to 2020, *Atmos. Environ.*, *44*(20), 2487–2499.

Selin, N. E., D. J. Jacob, R. M. Yantosca, S. Strode, L. Jaegle, and E. M. Sunderland (2008), Global 3-D land-ocean-atmosphere model for mercury: Present-day versus preindustrial cycles and anthropogenic enrichment factors for deposition, *Global Biogeochem. Cy.*, *22*, GB2011, doi:10.1029/2007GB003040.

Soerensen, A. L., E. M. Sunderland, C. D. Holmes, D. J. Jacob, R. M. Yantosca, H. Skov, J. H. Christensen, S. A. Strode, and R. P. Mason (2010), An improved global model for air-sea exchange of mercury: High concentrations over the North Atlantic, *Environ. Sci. Technol.*, *44*(22), 8574–8580.

Strode, S. A., L. Jaegle, N. E. Selin, D. J. Jacob, R. J. Park, R. M. Yantosca, R. P. Mason, and F. Slemr (2007), Air-sea exchange in the global mercury cycle, *Global Biogeochem. Cy.*, *21*(1), Art. No. GB1017.

Tseng, C. M., C. H. Lamborg, and W. F. Fitzgerald (2010), Development of a novel on-line flow injection mercury analyzer to determine gaseous elemental mercury over the northern South China Sea, *J. Anal. At. Spectro.*, *25*(4), 526–533.

Tseng, C. M., C. S. Liu, and C. H. Lamborg (2012), Seasonal changes in gaseous elemental mercury in relation to monsoon cycling over the northern South China Sea, *Atmos. Chem. Phys.*, *12*, 7341–7350, doi:10.5194/acp-12-7341-2012.

Tseng, C. M., P. H. Balcom, C. H. Lamborg, and W. F. Fitzgerald (2003), Dissolved elemental mercury investigations in Long Island Sound using on-line Au amalgamation-flow injection analysis, *Environ. Sci. Technol.*, *37*(6), 1183–1188.

Tseng, C. M., C. Lamborg, W. F. Fitzgerald, and D. R. Engstrom (2004), Cycling of dissolved elemental mercury in Arctic Alaskan lakes, *Geochim. Cosmochim. Acta*, *68*(6), 1173–1184.

Tseng, C. M., G. T. F. Wong, Lin, II, C. R. Wu, and K. K. Liu (2005), A unique seasonal pattern in phytoplankton biomass in low-latitude waters in the South China Sea, *Geophys. Res. Lett.*, *32*(8).

Tseng, C. M., G. T. F. Wong, W. C. Chou, B. S. Lee, D. D. Sheu, and K. K. Liu (2007), Temporal variations in the carbonate system in the upper layer at the SEATS station, *Deep-Sea Res. II*, *54*(14-15), 1448–1468.

Valiela, I. (1995), *Marine Ecological Processes*, 2nd ed., 686 pp., Springer, New York.

Wangberg, I., S. Schmolke, P. Schager, J. Munthe, R. Ebinghaus, and A. Iverfeldt (2001), Estimates of air-sea exchange of mercury in the Baltic Sea, *Atmos. Environ.*, *35*(32), 5477–5484.

Wanninkhof, R. (1992), Relationship between wind-speed and gas-exchange over the ocean, *J. Geophys. Res.*, *97*(C5), 7373–7382.

Xiao, Z. F., J. Munthe, W. H. Schroeder, and O. Lindqvist (1991), Vertical fluxes of volatile mercury over forest soil and lake surfaces in Sweden, *Tellus B*, *43*(3), 267–279.